

Tailoring Deep Eutectic Solvents to Provoke Solubility and Bioavailability of Naringin: Implications of a Computational Approach

Pankaj V. Dangre,* Pawan P. Korekar, Maheshkumar R. Borkar, Kaushalendra K. Chaturvedi, Sachin P. Borikar, and Anil M. Pethe



Cite This: *ACS Omega* 2023, 8, 12820–12829



Read Online

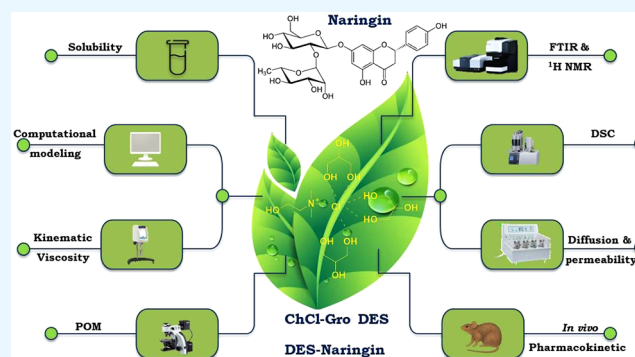
ACCESS |

Metrics & More

Article Recommendations

Supporting Information

ABSTRACT: Recently, the applications of deep eutectic solvents (DESs) as green and sustainable solvents for the solubilization of functional foods and phytophenols have dramatically risen concerning global issues on the utilization of organic solvents. Nevertheless, developing a suitable DES system for phytochemicals to enhance its solubility and bioavailability is complex and requires a sound experimental setup. Herein, we have attempted to develop DES encompassing the choline chloride (ChCl) along with oxalic acid (OA), L-glutamine (L-Glu), urea (U), and glycerol (Gro) at different ratios to elicit the solubility and bioavailability of naringin (NAR). Several DES systems were designed and tested for solubility, kinematic viscosity, and pH. Among these, DES-NAR encompassing ChCl/Gro in a 1:3 ratio exhibited the maximum solubility of NAR (232.56 ± 7.1 mg/mL) and neutral characteristic and thus considered suitable for NAR. Further, the conductor-like screening model for real solvents (COSMO-RS) has been employed to estimate the molecular and electrostatic interactions. DES-NAR was evaluated by polarized optical microscopy, Fourier-transform infrared (FTIR), differential scanning calorimetry (DSC), and ^1H NMR to investigate the molecular transition and interaction. Further, diffusion and permeability studies were performed, which suggest significant improvements in DES-NAR. Likewise, the pharmacokinetic studies revealed a two times increase in the oral bioavailability of NAR in a designed DES system. Thus, the work represents a systematic and efficient development of the DES system for a potential phytochemical considering the biosafety impact, which may widen the interest in pharmaceutical and food sciences.



1. INTRODUCTION

Naringin (NAR), chemically known as 4',5,7-trihydroxyflavone 7-rhamnoglucoside, is a flavonoid that copiously found in grapefruits and numerous citrus fruits belonging to the family *Rutaceae*, and it is a bitter compound synthesized through a shikimic acid pathway.¹ NAR is investigational proven to have multifarious pharmacologic activities and pharmacotherapeutic perspectives in modern medicine, for instance, anti-inflammatory,² antidiabetes,³ antitumor,⁴ congestive heart failure,⁵ metabolic disorders,⁶ neurodegenerative diseases,⁷ antirespiratory,⁸ etc. While NAR offers numerous clinical benefits, its application in clinical setup is restricted owing to poor oral bioavailability, i.e., 8.8% in preclinical and clinical models.⁹ The plausible reasons cited in the literature for low bioavailability encompass low aqueous solubility, low dissolution rate, low stability in gastric conditions, and oxidative vulnerability, which ultimately causes low absorption of NAR.^{10,11} Furthermore, it underwent an extensive phase I metabolism by a microbial enzyme, which also results in a low bioabsorption¹² and poses a challenge in its oral admin-

istration. Several attempts were made to surmount these critical matters, viz., polymeric nanoparticles,¹³ microspheres,¹⁴ solid dispersion,¹⁵ polymeric micelles,¹⁶ complexation,¹⁷ etc. However, implementing a more promising carrier that could address the solubility and bioavailability aspect of NAR should be designed and explored to gain maximum health benefits. The dose of NAR is 160 mg and has an elimination half-life of 3.64 ± 3.0 h.¹⁸ It has been established that NAR can inhibit the cytochrome P₄₅₀-3A4 or prevent P-glycoprotein-induced efflux, thereby lowering presystemic metabolism and increasing the bioavailability of drugs like paclitaxel and diltiazem.^{9,19,20}

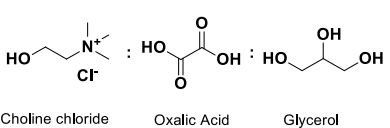
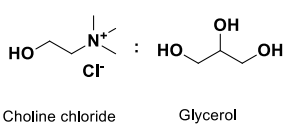
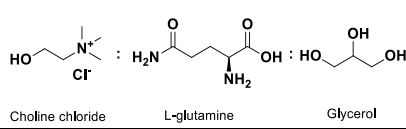
Received: December 20, 2022

Accepted: February 20, 2023

Published: March 30, 2023



Table 1. Characterization of Prepared DES-NAR Stable at Room Temperature

DESs	Molar ratio	Visual aspect at RT [#]	pH	Kinematic viscosity (cSt)	Solubility (mg/mL)
ChCl: OA: Gro  Choline chloride Oxalic Acid Glycerol	1:1:1	Light yellow viscous liquid	1.2 ± 0.1	71.34 ± 1.4	49.97 ± 2.5
	1:1:0.75	Light yellow viscous liquid	1.3 ± 0.4	73.43 ± 1.7	40.02 ± 2.2
	1:1:0.5	Light yellow viscous liquid	1.4 ± 0.2	67.27 ± 2.1	30.08 ± 2.1
ChCl: Gro  Choline chloride Glycerol	1:1	Transparent viscous liquid	5.8 ± 0.2	110.61 ± 3.2	210.60 ± 4.8
	1:2	Transparent viscous liquid	6.4 ± 0.1	99.85 ± 1.8	190.86 ± 6.2
	1:3	Transparent viscous liquid	6.3 ± 0.5	111.58 ± 2.2	232.56 ± 7.1
	2:1	Transparent viscous liquid	6.1 ± 0.1	113.47 ± 1.4	185.05 ± 5.4
	3:1	Transparent viscous liquid	6.2 ± 0.3	123.12 ± 2.5	160.94 ± 3.7
ChCl: L-Glu: Gro  Choline chloride L-glutamine Glycerol	1:1:1	Light yellow viscous liquid	5.2 ± 0.5	180.17 ± 2.5	169.72 ± 6.7
	1:2:1	Light yellow viscous liquid	5.1 ± 0.2	197.91 ± 3.7	140.84 ± 4.9
	1:3:1	Light yellow viscous liquid	5.6 ± 0.4	201.13 ± 3.1	130.58 ± 3.4

[#]RT[#]- All of the observations were noted at prevailing room temperature conditions.

Presently, the exploration of green solvents for the solubilization of promising phytophenols is attaining more interest because of their safety, low toxicity, and biodegradability.²¹ Further, green solvents, as a promising carrier for the solubilization of hydrophobic phytophenols, could be an exciting approach to green technology. Environmentally and economically sustainable systems are of special concern in these strategies.^{19,22} Deep eutectic solvents (DESs) have turned out as promising green solvent substitutes for ionic liquids (ILs) for the improvement of solubility and bioavailability.²³ However, DES also possesses a few drawbacks, such as low-to-moderate stability, high viscosity, hygroscopicity, and some extent of volatility. These factors should have been taken into consideration and addressed carefully during the design of DESs.²⁴

A DES is a modern category of solvent that is made up of a hydrogen bond acceptor (HBA) and a hydrogen bond donor (HBD) that can self-associate, primarily by interaction through a hydrogen bond, to shape out a eutectic combination having a lower melting point (typically exists in liquid form at temperatures <100 °C) than the basic components.^{25,26} The two molecules are joined by hydrogen bonds (specifically intermolecular), where the former serves as the HBA and the latter as the HBD. The charge delocalization mechanism caused by intermolecular hydrogen bonding has also been linked to the melting temperature drop when salt + HBD is mixed.^{26,27} DESs are desirable because they can be manufactured at a low cost while retaining high purity. DESs have many characteristics, including biodegradability, low

volatility, sustainability, ease of preparation, and the ability to tune their properties for a particular use.^{28,29} Further, DESs offer the promising capability to tune the dissolution, absorption, and permeation of a broad range of molecules, including phytophenols.^{30,31} The attentiveness to the exploitation of DESs in several disciplines, such as nutraceuticals, functional foods, and pharmaceuticals, has been tremendously growing. Hence, it is imperative to design DESs using a systematic experimental setup emphasizing solubility and bioavailability assessment. This approach could explore a new avenue in developing DESs with a thorough understanding and better utilization.

The presented work principally emphasized developing a novel DES system utilizing appropriate HBA and HBD ratios that would allow the increment in the solubility and bioavailability of NAR. The COSMOS-RS computational modeling tool was used to explore the solvation properties of DESs and to screen the NAR's solubility in various DESs.

2. MATERIALS AND METHODS

2.1. Materials. Naringin (≥95%) was procured from Sigma-Aldrich (Life Science) Ltd. Choline chloride, glycerol, and urea were acquired from Loba Chemie Ltd., Mumbai. L-glutamine was bought from Research Lab Ltd., Mumbai. All other chemicals utilized in this study were of analytical grade and procured from Himedia Ltd., Mumbai.

2.1.1. Preparation of DESs. DESs were prepared by combining ChCl as the HBA with a single or twin HBD, namely, oxalic acid (OA), L-glutamine (L-Glu), urea (U), and

glycerol (Gro) at various molar ratios, as shown in Table 1. Each of these mixers was placed in a glass vial and reacted at 80 °C on a heating plate with continued agitation until a transparent and uniform system was produced.²⁹ The DESs, which remained stable in a liquid state after 72 h of its preparations in ambient storage conditions, were characterized for physical properties, and stable DESs were utilized further for solubility determination.

2.1.2. Determination of Solubility. An excess quantity of NAR was placed in sealed vials comprising 2 mL of each DES and warmed in a constant temperature water bath at 40 °C for 5 min while stirring with a vortex mixer to help in the solubilization and then kept for 24 h to achieve equilibrium. The mixture was then centrifuged for 25 min at 26,916g. The upper clear liquid was separated and diluted with methanol to obtain an absorbance value in the linearity range. The amount of dissolved NAR was measured at a λ_{max} of 283 nm by employing a ultraviolet–visible (UV–vis) spectrophotometer (Shimadzu, UV-1900, Kyoto, Japan).³²

2.1.3. Computational Modeling. The computational modeling to investigate the solute–solvent interaction is of great importance. It is a predictive tool to discover the molecular mechanism and solvation behavior. Herein, the conductor-like screening model for real solvents (COSMO-RS) was utilized to predict NAR's molecular interactions and solvation behavior in the selected DESs. COSMO-RS is the most precise ab initio computational technique accessible to understand the molecular interactions among the solute and solvent.³³ It enables the computation of interaction energy among solvent and solute from the surface charge density (σ). The σ -profile allows in-depth data on molecular polarity and is regarded as a fingerprint of the molecule.³⁴ The σ -profile of DESs encompassing ChCl, Gro, and NAR was calculated using COSMO-RS software.

2.1.4. pH Measurements. The pH of DES encompassing NAR was determined with a pH meter (Systronics, India) at ambient conditions. A clean and dry beaker having a pH electrode was filled with 10 mL of DES sample and then the DES was left to become stable, and pH was recorded carefully.²¹

2.1.5. Estimation of Kinematic Viscosity. A rheometer (Brookfield Rheo 3000) was used to estimate the viscosity of DES-NAR. A sample probe CCT 40 connected to a rheometer spindle revolving at 100 rpm was filled with 60 mL of DES. The measured value was expressed in kinematic viscosity (cSt).^{21,35}

2.1.6. Polarized Optical Microscopy (POM). POM was performed to inspect the occurrence of microstructure in the DES sample. DES (plain), DES-NAR, and NAR (pure) in distilled water were dropped on a glass slide and visualized at 200 \times magnification. A DM 1000 microscope with a camera setup was used to monitor and film the polarized light picture at room temperature (Leica Biosystems).^{23,30}

2.1.7. Fourier-Transform Infrared (FTIR) Spectroscopy. The FTIR spectra for NAR (pure), DES (plain), and DES-NAR were obtained by employing an FTIR spectrophotometer (Shimadzu, FTIR-8400s, Kyoto, Japan) having a 2 cm^{-1} resolution. Each liquid sample was put in a sample holder and scanned throughout the 4000–400 cm^{-1} range.³⁶ NAR (pure) of about 2 mg was crushed with desiccated KBr in 1:100 ratio to obtain the fine powder and then transferred into the sample holder and scanned in similar conditions stated above.³⁷

2.1.8. Differential Scanning Calorimetry (DSC). DSC (Mettler Toledo, STARE-V 10.00) was taken into an application for determining the thermal attributes of NAR (pure), DES, and DES-NAR. In a typical aluminum pan with a nitrogen gas flow rate of 40 mL/min, each sample was warmed at a steady rate of 10 °C/min, and heat flow was settled at 0–300 °C.³⁰

2.1.9. Proton Nuclear Magnetic Resonance (¹H NMR). ¹H NMR investigation of NAR (pure), DES (plain), and DES-NAR was performed. A Bruker Avance Neo 500 MHz NMR spectrometer was used to record the ¹H NMR spectra using dimethyl sulfoxide-*d*₆ (DMSO-*d*₆) as a solvent at 298.15 K. The chemical shifts were recorded by employing tetramethylsilane as an internal standard. The following are the abbreviations for multiplicity: s, singlet; d, doublet; dd, doublet of doublet; t, triplet; m, multiplet.³⁸

2.1.10. Diffusion and Permeability Studies. The diffusion studies of NAR (pure) and DES-NAR were conducted using a diffusion cell apparatus (EDC-07, Electrolab, India). The donor and receptor compartments were segregated using a diffusion membrane (LA 395, Himedia Laboratories, India) having an effective surface area of 1.766 cm^2 and a diameter of 1.5 cm, which was washed and activated. The receptor compartment consists of phosphate-buffered saline (PBS) pH 6.8, kept under constant agitation of 50 rpm at 37 °C. Later, the donor compartment was filled with NAR (pure) and DES-NAR containing an equivalent amount of NAR (50 mg/mL). Aliquots of 500 μL were withdrawn from the receptor compartment at specified time intervals and were replenished with an adequate volume of the same medium kept at a similar condition to ascertain the sink conditions. The aliquots were filtered through a membrane filter with a 0.45 μm pore size (Millipore, India) and analyzed by a UV–vis spectrophotometer at a λ_{max} of 283 nm.^{21,39} The permeability of NAR (pure) and DES-NAR through the membrane was measured using the following formula

$$-\ln\left(1 - \frac{2C_t}{C_0}\right) = \frac{2A}{V} \times P \times t \quad (1)$$

where P is the permeability, C_t is the concentration of NAR in the receptor compartment, t is the time taken by the NAR to diffuse through the membrane, C_0 is the initial concentration of NAR in the donor compartment, A is the effective mass transfer area, and V is the volume of the medium in both compartments.³⁹

2.1.11. Pharmacokinetic Study. The DES-NAR and NAR (pure) suspensions (Na-CMC 0.5% w/v) were used in the pharmacokinetic study. The Institutional Animal Ethical Committee (IAEC) approved the animal study proposal (IAEC/RCPIPER/2020–21/18). Moreover, the National Institutes of Health (NIH) guideline for handling experimental animals (NIH Publications No. 8023, revised 1978) was stringently adopted throughout the experiment. Wistar male rats weighing 220–250 g and aged 10–12 weeks were housed in clean polypropylene cages under a normal environment (25–20 °C, 12 h light/dark cycle). Before the dosing, the rats abstained from feeding throughout the night and were given free admittance to water (ad libitum). Wistar rats were divided into two groups at random ($n = 6$). Group I was treated with NAR (pure) suspension (50 mg/kg), whereas group II was administered with DES-NAR at 50 mg/kg of NAR. Blood (0.5 mL) was removed from the retro-orbital vein at 0, 0.5, 2, 4, 6,

8, 12, and 24 h. Centrifugation at 10,000 rpm for 10 min was performed to sort out the plasma and then stored at $-18\text{ }^{\circ}\text{C}$ in a deep freezer. The plasma was precipitated utilizing acetonitrile in a 1:3 ratio (plasma to acetonitrile), followed by centrifugation at 5000 rpm for 5 min to separate the precipitate. An aliquot of supernatant liquid was made in the optimized mobile phase comprising acetonitrile and purified water (23:77 v/v %), pH-2.5, and quantified by employing an HPLC system (Agilent Tech.-1100) with a diode array detector. The chromatographic analysis was carried out at room temperature on a C18 column (Eclipse XDE). A flow rate of the mobile phase was maintained at 1 mL/min in an isocratic manner for 10 min as run time. About 20 μL of analyte was injected, and the amount of NAR was measured at 283 nm. The pharmacokinetic parameters of NAR (pure) and DES-NAR were estimated using pK solver software.

2.1.12. Statistical Analysis. All of the experimental findings were described as mean and standard deviation after being statistically validated. GraphPad Prism (ver. 4.0) software was utilized to assess the variation in the pharmacokinetic parameter among NAR (pure) and DES-NAR. The one-way analysis of variance (ANOVA) test was used to compare the diffusion profile, followed by a post hoc analysis. A probability (p) of 0.05 was considered significant.

3. RESULTS AND DISCUSSION

3.1. Preparation of DESs. The DESs have been prepared by employing different ratios of HBA and one or more HBD in varied ratios. DESs encompassing the ChCl and dual HBDs, i.e., OA and Gro in molar ratios of 1:1:1, 1:1:0.75, and 1:1:0.5, have remained as a yellow viscous liquid at room temperature after 72 h. DESs encompassing ChCl and Gro in all selected ratios, such as 1:1, 1:2, 1:3, 2:1, and 3:1, represent a clear liquid system at room temperature. Further, DESs comprising ChCl and U (3:1) and ChCl with L-Glu and Gro with molar ratios of 1:1:1, 1:2:1, and 1:3:1 remained stable liquid at ambient conditions. All of the selected ratios (Table 1) represent stability at normal room temperature conditions without any precipitation and solidification and hence utilized for further studies.

3.2. Determination of Solubility. The solubility of NAR in various prepared DESs that were stable liquids at room temperature is presented in Table 1. The DESs encompassing the ChCl as HBA and various HBDs in different ratios were prepared and tested. Among several DESs tested, NAR showed maximum solubility ($232.56 \pm 7.1\text{ mg/mL}$) in the DES system comprising ChCl/Gro having a molar ratio of 1:3, whereas the same DES with different molar ratios, i.e., 1:1, 1:2, 2:1, and 3:1, showed 210.60 ± 4.8 , 190.86 ± 6.2 , 185.05 ± 5.4 , and $160.94 \pm 3.7\text{ mg/mL}$. The DES system with ChCl/OA/Gro at molar concentrations of 1:1:1, 1:1:0.75, and 1:1:0.5 showed NAR solubility of 49.97 ± 2.5 , 40.02 ± 2.2 , and $30.08 \pm 2.1\text{ mg/mL}$, respectively. The DES system comprising ChCl/U at a molar ratio of 3:1 exhibited NAR solubility of $121.13 \pm 5.5\text{ mg/mL}$. The solubility of the DES system with ChCl/L-Glu/Gro in molar ratios of 1:1:1, 1:2:1, and 1:3:1 was 169.72 ± 6.7 , 140.84 ± 4.9 , and $130.58 \pm 3.4\text{ mg/mL}$, respectively. Hence, the DES comprising ChCl/Gro in a ratio of 1:3 (Figure 1) was selected owing to the optimum solubility of NAR. The strong intermolecular hydrogen bonding and neutral nature of DESs suggest the main driving force for the solubilization of NAR.

3.3. Computational Modeling. The most important feature in COSMOS-RS computation modeling is to have

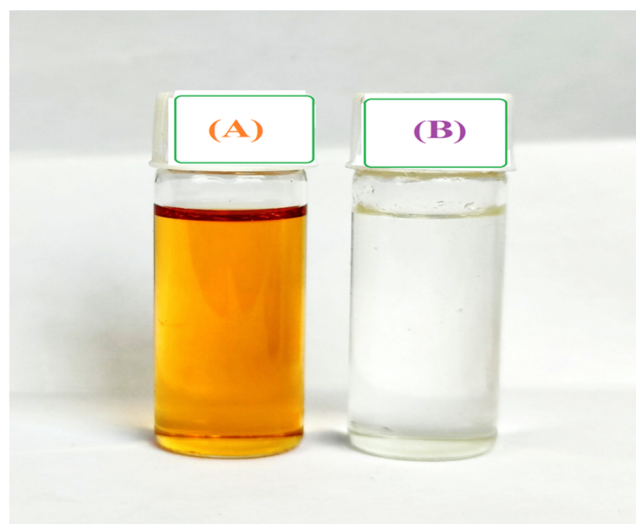


Figure 1. Appearance of prepared DESs comprising ChCl/Gro (1:3). (A) DES system containing NAR. (B) DES system without NAR. Both the systems indicate the homogeneous mixtures.

charge distribution (σ) over the molecular surface. The σ -profile histogram is employed to calculate interaction energy and electrostatic interactions between the molecular compounds based on possible hydrogen bonds. Further, this study helps to predict the behavior of compounds in a system. The σ -profiles of ChCl, Gro, and NAR molecules are depicted in Figure 2. The σ -profile histogram was categorized into three

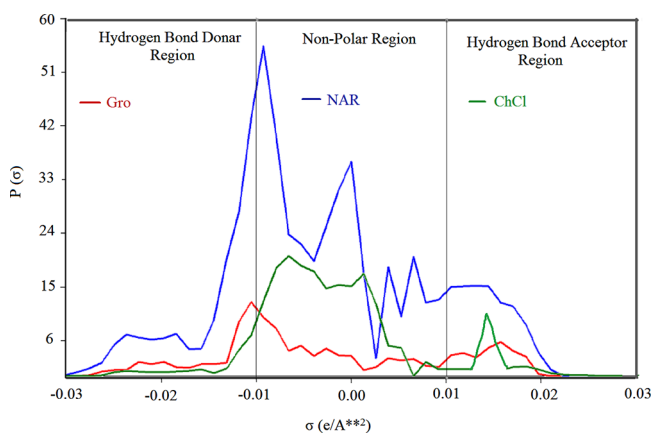
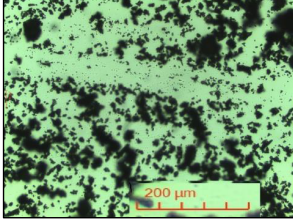
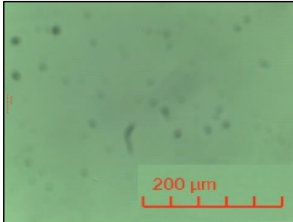
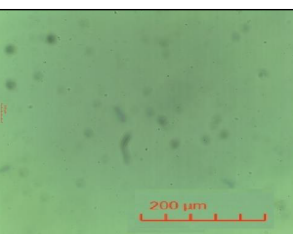


Figure 2. σ -profiles of Gro, NAR, and ChCl.

regions viz., hydrogen bond donor, nonpolar region, and hydrogen bond acceptor. The prominent surface area of NAR in the nonpolar region (-0.01 and $+0.01\text{ e/A}^2$) indicates high hydrophobicity. The σ -profile of Gro in the hydrogen bond donor region represents its ability to form strong hydrogen bonds. Moreover, the σ -profile of ChCl indicates positive charge densities owing to the presence of quaternary ammonium salts in the structure showing hydrogen bond acceptor behavior. Therefore, Gro and ChCl on mixing resulted in a favorable intermolecular interaction. The molecular interaction leads to form strong hydrogen bonding, which favors improvement in the solvation capacity of NAR.

3.4. pH Measurements. The pH of DESs depends on the functional group and nature of HBA and HBD.²¹ Table 1 displays the observed pH values for different DESs. The DESs

Table 2. Polarized Optical Microscopy (POM) Images of NAR (pure), DES (plain), and DES-NAR

DESs/Samples	Polarized Optical Microscopy
[#] NAR (Pure)	
[*] DES (Blank) (ChCl: Gro: 1:3)	
[§] DES-NAR (ChCl: Gro: 1:3)	

^aNAR (pure) raw powder added in a suitable amount of water. ^bDES (blank) selected preparation without NAR. ^cDES-NAR selected preparation with NAR (232.56 ± 7.1 mg/mL).

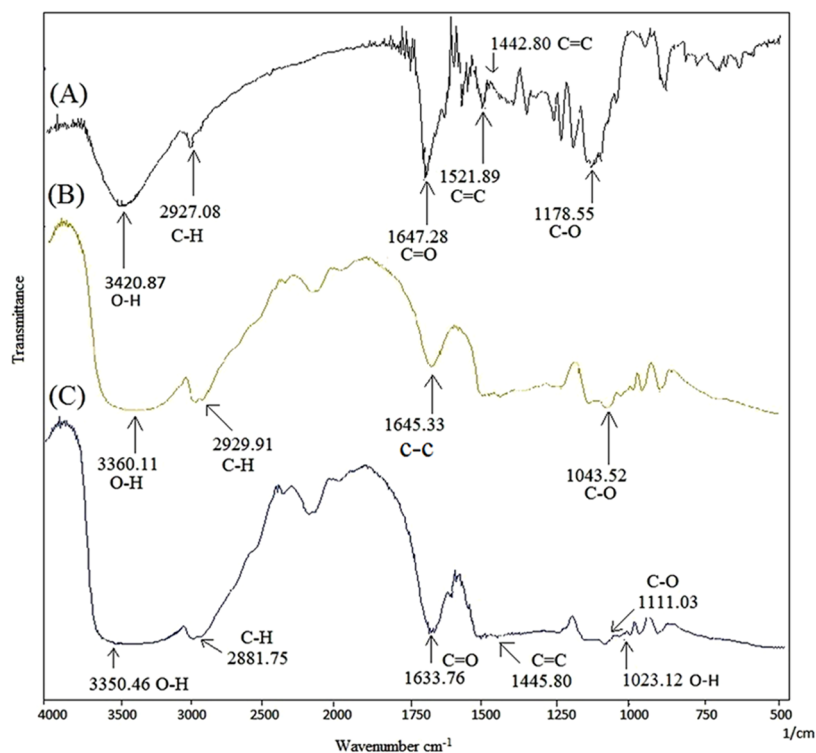


Figure 3. Fourier-transform infrared spectra of (A) NAR (pure), (B) DESs (plain), and (C) DES-NAR.

comprising ChCl/OA/Gro were highly acidic with a pH range of 1.2 ± 0.1 to 1.4 ± 0.2 . While the DESs of ChCl/Gro and

ChCl/L-Glu/Gro exhibited a pH from 5.1 ± 0.2 to 6.4 ± 0.1 , indicating a mildly acidic character. The DESs comprising

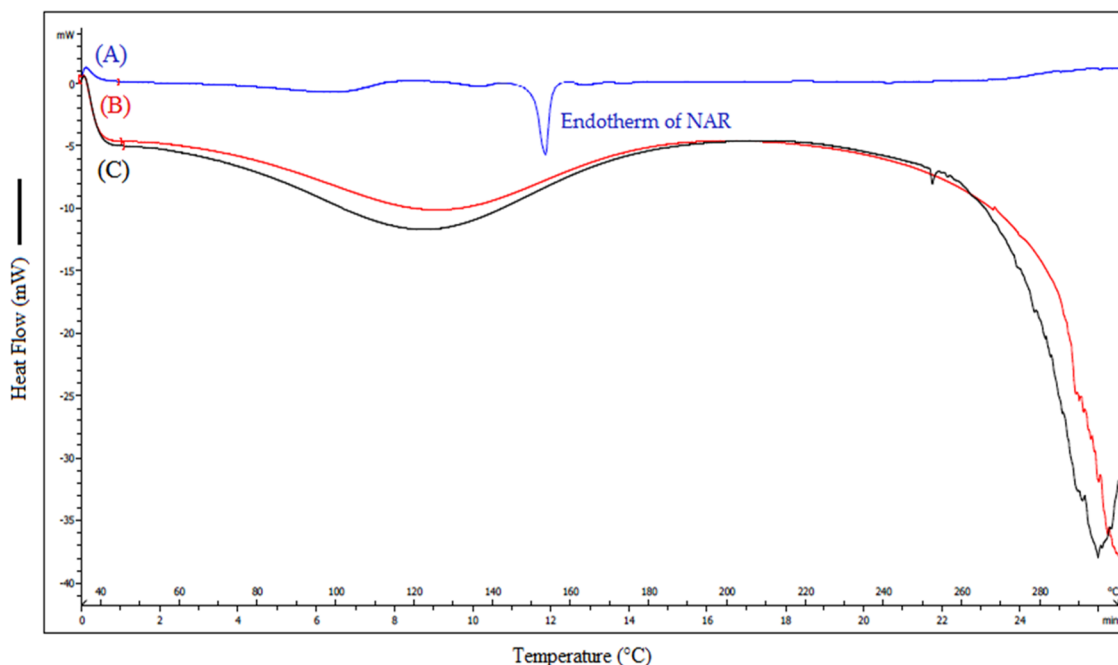


Figure 4. Differential scanning calorimetric (DSC) thermogram of (A) NAR (pure), (B) DESs (plain), and (C) DESs-NAR.

ChCl/U showed alkaline characteristics ($\text{pH} = 9.1 \pm 0.3$) due to the presence of the amine group.

3.5. Estimation of Kinematic Viscosity. The kinematic viscosity(s) of the developed DES-NAR are displayed in Table 1. The DES-NAR comprising ChCl/OA/Gro showed relatively lower viscosity ranges (67.27 ± 2.1 to 73.43 ± 1.7 cSt). On the contrary, DES-NAR constituting ChCl/L-Glu/Gro indicates high viscosity (180.17 ± 2.5 to 201.13 ± 3.1 cSt) owing to strong electrostatic interactions,²¹ while the DES-NAR comprising ChCl/Gro showed an intermediate viscosity range (99.85 ± 1.8 to 123.12 ± 2.5 cSt), revealing ideal behavior.

3.6. Polarized Optical Microscopy (POM). The presence of crystals or microstructure in the prepared NAR (pure) in water, DES (plain), and DES-NAR can be identified by POM. The images captured for different samples are illustrated in Table 2. The NAR (pure), when added to water and observed under a polarized microscope, it revealed the presence of crystalline particles. Visual examination revealed small crystals in a solvent, indicating the poor solubility of NAR in water. The results of POM analysis were very similar to the results of visual observations. The POM of the selected DES (plain) demonstrated a consistent green color image with no visible crystals in the medium; visually, it looked like a clear homogeneous solvent. Meanwhile, a visual examination and POM of DES-NAR revealed a clear liquid with no visible crystals, implying that the DES can keep the NAR in an extremely solubilized state and permit excellent solubilization capability.

3.7. FTIR Spectroscopy. FTIR spectra of NAR (pure), DES (plain), and NAR-DES are superimposed and presented in Figure 3. The NAR (pure) (Figure 3A) encompasses polyhydroxy groups, and thus, it exhibits the characteristic peaks at 3420.87 cm^{-1} owing to $-\text{OH}$ stretching; the peak at 2927.08 cm^{-1} was attributed to $\text{C}-\text{H}$ stretching vibrations. A signal at 1647.28 cm^{-1} indicates the stretching vibrations of the carbonyl $\text{C}=\text{O}$ group, while in the aromatic ring, the signals at 1521.89 and 1442.80 cm^{-1} represent the $\text{C}=\text{C}$ vibrations. The

signals at 1297.17 , 1178.55 , and 1136.11 cm^{-1} represent $\text{C}-\text{O}$ stretching vibrations. The observations were close to those previously reported in the literature.^{1,13} DES (plain) (Figure 3B) exhibited the absorption bands at 3360.11 cm^{-1} ($\text{O}-\text{H}$, stretching), 2929.91 cm^{-1} ($\text{C}-\text{H}$, stretching), 1645.33 cm^{-1} ($\text{C}-\text{C}$, stretching), and 1043.52 cm^{-1} ($\text{C}-\text{O}$, stretching). DES-NAR (Figure 3C) reveals prominent absorption bands at 3350.46 cm^{-1} ($\text{O}-\text{H}$, stretching), 2881.75 cm^{-1} ($\text{C}-\text{H}$, stretching), and 1633.76 cm^{-1} ($\text{C}=\text{O}$, stretching), which are corroborated with the development of DES. Further, the prominent signals pertinent to NAR (pure) were found at absorption bands of 1445.80 cm^{-1} of $\text{C}=\text{C}$ vibrations, 1111.03 cm^{-1} of $\text{C}-\text{O}$ stretching, and 1023.12 cm^{-1} ascribed to $\text{O}-\text{H}$ in-plane deformation, revealing that the DES contains NAR in the dissolved state having good solubilization capacity.

3.8. Differential Scanning Calorimetry (DSC). DSC thermograms of NAR (pure), DES (plain), and DES-NAR are depicted in Figure 4. The NAR (pure) (Figure 4A) shows endothermic peaks between the ranges of 150 to $170 \text{ }^\circ\text{C}$ ($T_{\text{onset}} = 157.33 \text{ }^\circ\text{C}$, $T_{\text{peak}} = 162.92 \text{ }^\circ\text{C}$, and $T_{\text{endset}} = 169.94 \text{ }^\circ\text{C}$). The observations were similar to the previously reported literature.¹³ The crystalline structure of NAR is confirmed by its endothermic peak. The DES (plain) (Figure 4B) exhibited a broad and diffused peak, indicating the neat solvent characteristics. Moreover, the DES-NAR (Figure 4C) exhibited a similar observation pertinent to DES (plain), showing the broad and diffused peak. The absence of endotherm suggested the polymorphic transition of NAR in the prepared DES, which further confers the capacity of DES to improve the solubilization of NAR due to the transformation of crystalline to an amorphous state.

3.9. ^1H NMR. The ^1H NMR spectra of NAR (pure), DES (plain) and DES-NAR are illustrated in Figure 5. The ^1H NMR spectrum of NAR (pure) (Figure 5A) shows the following signals: $\delta = 12.07$ (s, 1H, 33); 9.64 (s, 1H, 35); $7.34-7.32$ (m, 2H, 2', 6'); $6.81-6.79$ (m, 2H, 3', 5'); $6.12-6.11$ (dd, 1H, 6); $6.09-6.08$ (dd, 1H, 8); $5.53-5.47$ (t, 1H, 2);

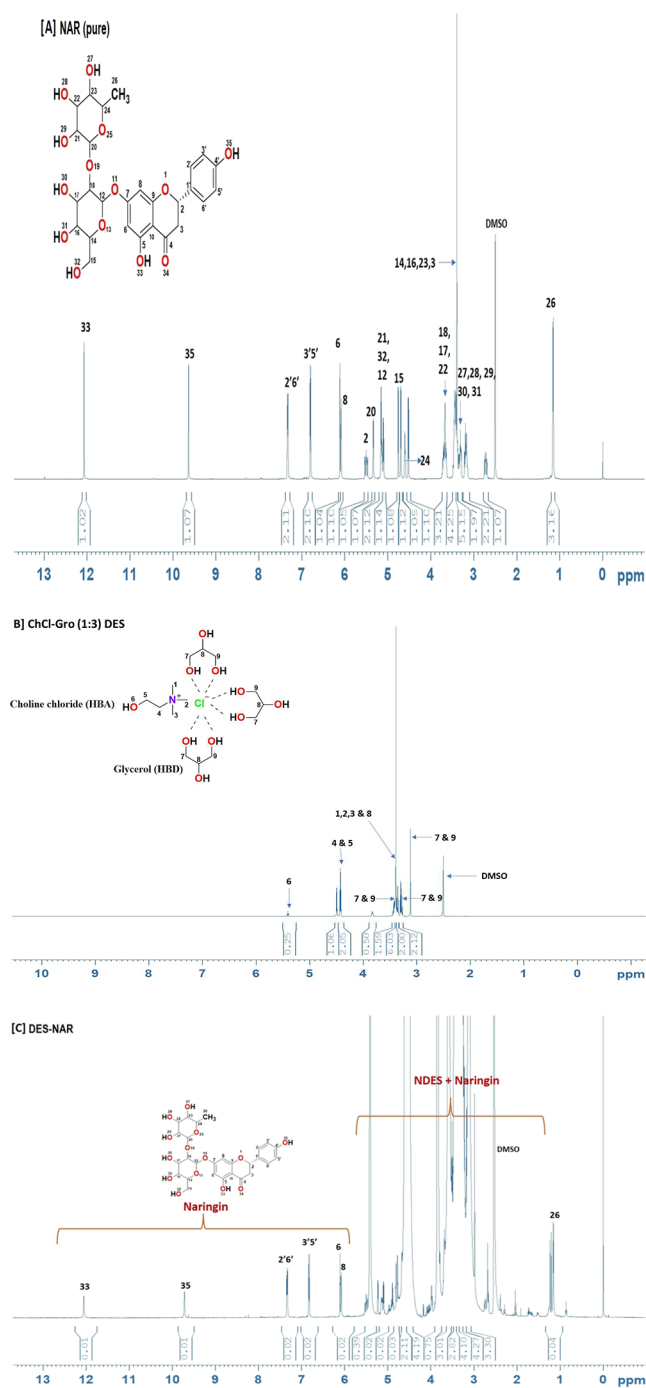


Figure 5. ^1H Nuclear magnetic resonance (NMR) spectra of (A) NAR (pure), (B) DESs (plain), and (C) DESs-NAR.

5.34 (d, 1H, 20); 5.16 (m, 1H, 21); 5.13 (s, 1H, 32); 5.12 (d, 1H, 12); 4.7 (d, 1H, 15); 4.5 (d, 1H, 15); 4.6 (m, 1H, 24); 3.72–3.64 (s, 1H, 18); 3.72–3.64 (s, 1H, 17); 3.72–3.64 (s, 1H, 22); 3.48–3.41 (m, 1H, 14); 3.48–3.41 (m, 1H, 16); 3.48–3.41 (m, 1H, 23); 3.22 (m, 2H, 3); 3.40 (s, 6H, 27, 28, 29, 30, 31); 1.16 (dd, 3H, 26). In the ^1H NMR spectrum of DES (plain) (Figure 5B), the signals of the three-methyl group (1, 2, 3) bonded to the choline nitrogen, $(\text{CH}_3)_3\text{N}^+$, and 8-H of Gro are overlapping; however, the rest are well separated: $\delta = 4.43\text{--}4.41$ (t, 4H, 4,5); 3.39 (s, 3H, 1); 3.39 (s, 3H, 2); 3.39 (s, 3H, 3); 3.41–3.38 (m, 3H, 8); 3.44–3.41 (m, 4H, 7, 9); 3.37–3.34 (m, 4H, 7, 9); 3.31–3.26 (m, 4H, 7, 9). The

nonexistence of the hydroxyl (OH) peak of Gro in DES spectra affirmed the intermolecular hydrogen bonding involving ChCl and Gro. The plausible chemical intervention among ChCl and Gro is depicted in Figure 5B. NMR spectra of DES-NAR preparation (Figure 5C) showed the presence of chemical shift of NAR at $\delta = 7.34\text{--}7.32$ (m, 2H, 2', 6') and 6.83–6.81 (m, 2H, 3', 5') for the aromatic region. Also, it shows the presence of 33-OH and 35-OH at $\delta = 12.05$ and 9.72, respectively. Similarly, the occurrences of chemical shift $\delta = 6.11\text{--}6.08$ (dd, 1H, 6), 6.08–6.07 (dd, 1H, 8), and 1.23 (dd, 3H, 26) and the peaks of DES overlapped with the NAR peaks confirm the presence of NAR in the DES. The individual ^1H NMR spectra of NAR (pure), DES (plain), and DES-NAR are displayed in Figures S1, S2, and S3 (Supporting Material).

3.10. Diffusion and Permeability Studies. The diffusion profile of NAR (pure) and DES-NAR is presented in Figure 6.

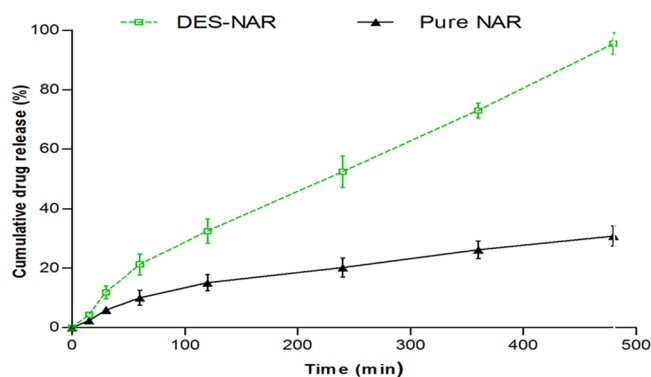


Figure 6. Diffusion of NAR powder and DES-NAR in phosphate buffer medium (pH 6.8) after 480 min.

The amount of NAR diffused after 480 min in prepared DES-NAR was found to be $95.47 \pm 3.60\%$ w/v. In contrast, NAR (pure) showed significantly less diffusion, i.e., $30.78 \pm 3.4\%$ w/v after 480 min. The diffusion was found to be much higher in DES-NAR due to an enhancement in the solubility of NAR in the DES. The Higuchi mechanism ($r^2 = 0.997$), which governs the Fickian motion of molecules with a result exponent (n) of less than 0.5, was predominantly responsible for the diffusion of NAR. The permeability of NAR was estimated through comparison among different systems and expressed as permeability coefficient k , (cm s^{-1}). The k was estimated according to Fick's law and found to increase in DES-NAR than in NAR (pure). The k value for DES-NAR was significantly more, i.e., 2.204 ± 1.8 ($10^{-6} \text{ cm s}^{-1}$) than NAR (pure), having 1.421 ± 1.5 ($10^{-6} \text{ cm s}^{-1}$) after 480 min (Table S1, Supporting Material), suggesting an increment in the permeability of NAR in the developed DES.

3.11. Pharmacokinetic Study. The in vivo pharmacokinetic study of DES-NAR formulation was compared to NAR (pure). Figure 7 depicts the plasma concentration of NAR vs time (h) after oral administration of DES-NAR and NAR (pure) suspensions. The pharmacokinetic parameters were estimated by noncompartmental analysis of plasma data after extracellular input by the linear trapezoidal method, and observations are displayed in Table 3. The results showed that DES-NAR had higher AUC and C_{max} values than NAR (pure), which significantly corroborated NAR absorption's augmentation in the DES. Moreover, the T_{max} , half-life ($t_{1/2}$), and MRT increased significantly in the DES, indicating a substantial enhancement in NAR absorption due to the more solubiliza-

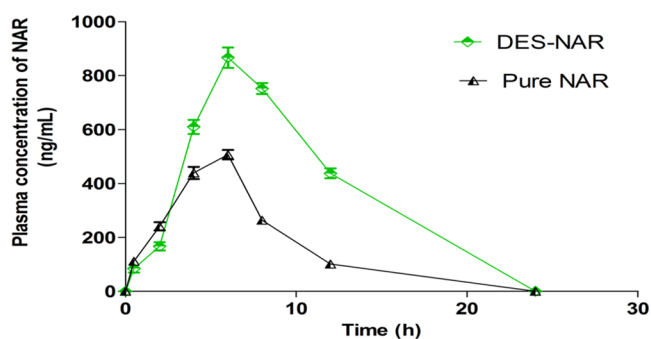


Figure 7. Plasma NAR concentration versus time (h) profile after oral administration of NAR suspension and DES-NAR.

Table 3. Pharmacokinetic Parameters for Pure NAR and DES-NAR^{a,b,c}

pharmacokinetic parameters	NAR (pure)	DES-NAR
AUC _{0-t} (ng/mL*h)	226.367 ± 4.2**	466.325 ± 7.2**
C _{max} (ng/mL)	31.24 ± 2.3**	53.41 ± 4.1**
T _{max} (h)	4.1 ± 0.6*	3.2 ± 0.8*
t _{1/2} (h)	3.43 ± 1.1*	4.12 ± 1.5*
MRT (h)	6.46 ± 1.7**	8.28 ± 2.2**
relative bioavailability (%)		206.00

^aMean ± SD (*n* = 6), Significant difference at *p* < 0.05, **Significant difference at *p* < 0.01. ^bAUC_{0-t}—Area under curve until last observation, C_{max}—Peak of maximum concentration. ^cT_{max}—Time of peak concentration, t_{1/2}—Elimination half-life, MRT—Mean residence time.

tion potentiality of the prepared DES. According to the literature, the poor water solubility of NAR is a likely cause for its low oral bioavailability. Here, an ameliorated oral absorption of NAR in the DES system resulted due to improved solubility and dissolution, leading to an increment in oral bioavailability. The relative bioavailability of DES-NAR was determined to be 206.0%, suggesting a more than the two times increase in NAR oral bioavailability.

4. CONCLUSIONS

The present study reports the development of DES for NAR encompassing ChCl as HBA and Gro as HBD. The developed DES showed good stability at room temperature conditions and excellent solubility of NAR. COSMOS-RS helps to elucidate the molecular interactions in the DES. NAR is reported to highly dissolved state in the developed DES, according to FTIR and DSC studies. ¹H NMR studies reveal intermolecular hydrogen bonding between DES and NAR. The diffusion and permeability were augmented in the DES, leading to improved NAR absorption, and therefore, a pharmacokinetic study further confirms the effectiveness of DES in increasing NAR oral bioavailability. The work presented is a proof-of-concept that may open up new avenues in food and pharmaceutical science for developing a more efficient and potential carrier system for promising phytophenols.

■ ASSOCIATED CONTENT

SI Supporting Information

The Supporting Information is available free of charge at <https://pubs.acs.org/doi/10.1021/acsomega.2c08079>.

Proposed HPLC method for the determination of NAR in rat plasma was found to be linear in the concentration

over a range of 0.05–6 μg/mL with a regression coefficient (*r*²) = 0.997 and the equation was *Y* = 0.6155*x* + 0.006; the retention time of NAR and internal standard (IS) was 10.153 and 12.561 min, respectively (Figure S4). At these retention points, there was no interference of any substance in plasma. The LOD of NAR was found to be 5 ng/mL and LLOQ was 11 ng/mL. The proposed method was found to be rapid, specific, and reproducible for determination of NAR in rat plasma; ¹H NMR of naringin, NAR (pure); ¹H NMR of DES (plain); ¹H NMR of DES-NAR; permeability coefficient of NAR (pure) and DES-NAR; representative chromatogram of NAR with internal standard (IS) showing retention times 10.153 min and 12.561 min (PDF)

■ AUTHOR INFORMATION

Corresponding Author

Pankaj V. Dangre — Department of Pharmaceutics, Datta Meghe College of Pharmacy, DMIHER (DU), Wardha 442001 Maharashtra, India; Department of Pharmaceutical Quality Assurance, R C Patel Institute of Pharmaceutical Education and Research, Shirpur 425405 Maharashtra, India; orcid.org/0000-0003-4750-9384; Phone: +91-9960160479; Email: pankaj_dangre@rediffmail.com

Authors

Pawan P. Korekar — Department of Pharmaceutical Quality Assurance, R C Patel Institute of Pharmaceutical Education and Research, Shirpur 425405 Maharashtra, India

Maheshkumar R. Borkar — Department of Pharmaceutical Chemistry, SVKM's Dr. Bhanuben Nanavati College of Pharmacy, Mumbai 400056 Maharashtra, India

Kaushalendra K. Chaturvedi — Arnold and Marie Schwartz College of Pharmacy and Health Sciences, Long Island University, Brooklyn, New York 11201, United State

Sachin P. Borikar — Department of Pharmacology, Rajarshi Shahu College of Pharmacy, Buldana 443001 Maharashtra, India

Anil M. Pethe — Department of Pharmaceutics, Datta Meghe College of Pharmacy, DMIHER (DU), Wardha 442001 Maharashtra, India

Complete contact information is available at:

<https://pubs.acs.org/10.1021/acsomega.2c08079>

Notes

The authors declare no competing financial interest.

■ ACKNOWLEDGMENTS

The authors are grateful to the management of R C Patel Institute of Pharmaceutical Education and Research, Shirpur, India, and Datta Meghe College of Pharmacy, DMIHER (DU), Wardha, for providing the necessary equipment for this study. They would also like to thank STIC (Sophisticated Test and Instrumentation Centre) in Chandigarh, India, for conducting the sample analysis.

■ REFERENCES

- (1) Nallamuthu, I.; Ponnusamy, V.; Smruthi, M. R.; Khanum, F. Formulation of Naringin Encapsulation in Zein/Caseinate Biopolymers and Its Anti-Adipogenic Activity in 3T3-L1 Pre-Adipocytes. *J. Cluster Sci.* **2021**, *32*, 1649–1662.

- (2) Ahmad, S. F.; Attia, S. M.; Bakheet, S. A.; Zoheir, K. M. A.; Ansari, M. A.; Korashy, H. M.; Abdel-Hamied, H. E.; Ashour, A. E.; Abd-Allah, A. R. A. Naringin Attenuates the Development of Carrageenan-Induced Acute Lung Inflammation Through Inhibition of NF- κ B, STAT3 and Pro-Inflammatory Mediators and Enhancement of I κ B α and Anti-Inflammatory Cytokines. *Inflammation* **2015**, *38*, 846–857.
- (3) Zeng, X.; Su, W.; Zheng, Y.; He, Y.; He, Y.; Rao, H.; Peng, W.; Yao, H. Pharmacokinetics, Tissue Distribution, Metabolism, and Excretion of Naringin in Aged Rats. *Front. Pharmacol.* **2019**, *10*, No. 34.
- (4) Choi, E. J.; Lee, J. I.; Kim, G. Effects of 4',7-dimethoxyflavanone on cell cycle arrest and apoptosis in human breast cancer MCF-7 cells. *Arch. Pharmacol. Res.* **2011**, *34*, 2125–2130.
- (5) Alam, M. A.; Kauter, K.; Brown, L. Naringin Improves Diet-Induced Cardiovascular Dysfunction and Obesity in High Carbohydrate, High Fat Diet-Fed Rats. *Nutrients* **2013**, *5*, 637–650.
- (6) Alam, M. A.; Subhan, N.; Rahman, M. M.; Uddin, S. J.; Reza, H. M.; Sarker, S. D. Effect of Citrus Flavonoids, Naringin and Naringenin, on Metabolic Syndrome and Their Mechanisms of Action. *Adv. Nutr.* **2014**, *5*, 404–417.
- (7) Gopinath, K.; Sudhandiran, G. Protective Effect of Naringin on 3-Nitropropionic Acid-Induced Neurodegeneration through the Modulation of Matrix Metalloproteinases and Glial Fibrillary Acidic Protein. *Can. J. Physiol. Pharmacol.* **2016**, *94*, 65–71.
- (8) Gao, S.; Li, P.; Yang, H.; Fang, S.; Su, W. Antitussive Effect of Naringin on Experimentally Induced Cough in Guinea Pigs. *Planta Med.* **2011**, *77*, 16–21.
- (9) Lavrador, P.; Gaspar, V. M.; Mano, J. F. Bioinspired Bone Therapies Using Naringin: Applications and Advances. *Drug Discovery Today* **2018**, *23*, 1293–1304.
- (10) Hu, M. Commentary: Bioavailability of Flavonoids and Polyphenols: Call to Arms. *Mol. Pharmaceutics* **2007**, *4*, 803–806.
- (11) Sansone, F.; Aquino, R. P.; Del Gaudio, P.; Colombo, P.; Russo, P. Physical Characteristics and Aerosol Performance of Naringin Dry Powders for Pulmonary Delivery Prepared by Spray-Drying. *Eur. J. Pharm. Biopharm.* **2009**, *72*, 206–213.
- (12) Chen, T.; Su, W.; Yan, Z.; Wu, H.; Zeng, X.; Peng, W.; Gan, L.; Zhang, Y.; Yao, H. Identification of Naringin Metabolites Mediated by Human Intestinal Microbes with Stable Isotope-Labeling Method and UFLC-Q-TOF-MS/MS. *J. Pharm. Biomed. Anal.* **2018**, *161*, 262–272.
- (13) Mohanty, S.; Konkimalla, V. B.; Pal, A.; Sharma, T.; Si, S. C. Naringin as Sustained Delivery Nanoparticles Ameliorates the Anti-Inflammatory Activity in a Freund's Complete Adjuvant-Induced Arthritis Model. *ACS Omega* **2021**, *6*, 28630–28641.
- (14) Ghosal, K.; Ghosh, D.; Das, S. K. Preparation and Evaluation of Naringin-Loaded Polycaprolactone Microspheres Based Oral Suspension Using Box-Behnken Design. *J. Mol. Liq.* **2018**, *256*, 49–57.
- (15) Wang, J.; Ye, X.; Lin, S.; Liu, H.; Qiang, Y.; Chen, H.; Jiang, Z.; Zhang, K.; Duan, X.; Xu, Y. Preparation, Characterization and in Vitro and in Vivo Evaluation of a Solid Dispersion of Naringin. *Drug Dev. Ind. Pharm.* **2018**, *44*, 1725–1732.
- (16) Mohamed, E.; Hashim, I. A.; Yusif, R.; Shaaban, A.; El-Sheakh, A.; Hamed, M.; Badria, F. Polymeric Micelles for Potentiated Antulcer and Anticancer Activities of Naringin. *Int. J. Nanomed.* **2018**, *13*, 1009–1027.
- (17) Pai, D. A.; Vangala, V. R.; Ng, J. W.; Ng, W. K.; Tan, R. B. H. Resistant Maltodextrin as a Shell Material for Encapsulation of Naringin: Production and Physicochemical Characterization. *J. Food Eng.* **2015**, *161*, 68–74.
- (18) Bai, Y.; Peng, W.; Yang, C.; Zou, W.; Liu, M.; Wu, H.; Fan, L.; Li, P.; Zeng, X.; Su, W. Pharmacokinetics and Metabolism of Naringin and Active Metabolite Naringenin in Rats, Dogs, Humans, and the Differences Between Species. *Front. Pharmacol.* **2020**, *11*, No. 364.
- (19) Musmade, K. P.; Trilok, M.; Dengale, S. J.; Bhat, K.; Reddy, M. S.; Musmade, P. B.; Udupa, N. Development and Validation of Liquid Chromatographic Method for Estimation of Naringin in Nano-formulation. *J. Pharm.* **2014**, *2014*, 1–8.
- (20) Choi, J. S.; Shin, S. C. Enhanced Paclitaxel Bioavailability after Oral Coadministration of Paclitaxel Prodrug with Naringin to Rats. *Int. J. Pharm.* **2005**, *292*, 149–156.
- (21) Borase, H. P.; Borkar, M. R.; Chaturvedi, K. K.; Mahapatra, D. K.; Chalikwar, S. S.; Dangre, P. V. Design and Evaluation of Natural Deep Eutectic Solvents System for Chrysin to Elicit Its Solubility, Stability, and Bioactivity. *J. Mol. Liq.* **2022**, *345*, No. 118205.
- (22) Jeliński, T.; Przybyłek, M.; Cysewski, P. Solubility Advantage of Sulfanilamide and Sulfacetamide in Natural Deep Eutectic Systems: Experimental and Theoretical Investigations. *Drug Dev. Ind. Pharm.* **2019**, *45*, 1120–1129.
- (23) Silva, J. M.; Reis, R. L.; Paiva, A.; Duarte, A. R. C. Design of Functional Therapeutic Deep Eutectic Solvents Based on Choline Chloride and Ascorbic Acid. *ACS Sustainable Chem. Eng.* **2018**, *6*, 10355–10363.
- (24) Chen, Y.; Mu, T. Revisiting Greenness of Ionic Liquids and Deep Eutectic Solvents. *Green Chem. Eng.* **2021**, *2*, 174–186.
- (25) Zhang, Q.; De Oliveira Vigier, K.; Royer, S.; Jérôme, F. Deep Eutectic Solvents: Syntheses, Properties and Applications. *Chem. Soc. Rev.* **2012**, *41*, 7108–7146.
- (26) García, G.; Atilhan, M.; Aparicio, S. An Approach for the Rationalization of Melting Temperature for Deep Eutectic Solvents from DFT. *Chem. Phys. Lett.* **2015**, *634*, 151–155.
- (27) Aroso, I. M.; Paiva, A.; Reis, R. L.; Duarte, A. R. C. Natural Deep Eutectic Solvents from Choline Chloride and Betaine – Physicochemical Properties. *J. Mol. Liq.* **2017**, *241*, 654–661.
- (28) Morrison, H. G.; Sun, C. C.; Neervannan, S. Characterization of Thermal Behavior of Deep Eutectic Solvents and Their Potential as Drug Solubilization Vehicles. *Int. J. Pharm.* **2009**, *378*, 136–139.
- (29) Cysewski, P.; Jeliński, T. Optimization, Thermodynamic Characteristics and Solubility Predictions of Natural Deep Eutectic Solvents Used for Sulfonamide Dissolution. *Int. J. Pharm.* **2019**, *570*, No. 118682.
- (30) Aroso, I. M.; Silva, J. C.; Mano, F.; Ferreira, A. S. D.; Dionísio, M.; Sá-Nogueira, I.; Barreiros, S.; Reis, R. L.; Paiva, A.; Duarte, A. R. C. Dissolution Enhancement of Active Pharmaceutical Ingredients by Therapeutic Deep Eutectic Systems. *Eur. J. Pharm. Biopharm.* **2016**, *98*, 57–66.
- (31) Sut, S.; Faggian, M.; Baldan, V.; Poloniato, G.; Castagliuolo, I.; Grabnar, I.; Perissutti, B.; Brun, P.; Maggi, F.; Voinovich, D.; Peron, G.; Dall'Acqua, S. Natural Deep Eutectic Solvents (NADES) to Enhance Berberine Absorption: An in Vivo Pharmacokinetic Study. *Molecules* **2017**, *22*, No. 1921.
- (32) Nagarajana, S.; Murthy, T. E. G. K.; Rao, A. S. Solubility Data of Naringin and Rutin in Different Ph Media Using Uv Visible Spectrophotometer. *J. Pharm. Sci. Innov.* **2016**, *5*, 63–65.
- (33) Palmelund, H.; Andersson, M. P.; Asgreen, C. J.; Boyd, B. J.; Rantanen, J.; Löbmann, K. Tailor-Made Solvents for Pharmaceutical Use? Experimental and Computational Approach for Determining Solubility in Deep Eutectic Solvents (DES). *Int. J. Pharm.: X* **2019**, *1*, No. 100034.
- (34) Nabi, A.; Zain, S. B. M.; Jesudason, C. G. Densities, Ultrasonic Speeds, Refractive Indices, and COSMO Analysis for Binary Mixtures of Dichloromethane with Acetone and Dimethylsulfoxide at T = (298.15, 303.15, and 308.15) K. *Chem. Eng. Commun.* **2018**, *205*, 479–491.
- (35) Jangir, A. K.; Lad, B.; Dani, U.; Shah, N.; Kuperkar, K. In Vitro Toxicity Assessment and Enhanced Drug Solubility Profile of Green Deep Eutectic Solvent Derivatives (DESDs) Combined with Theoretical Validation. *RSC Adv.* **2020**, *10*, 24063–24072.
- (36) Al-Akayleh, F.; Ali, H. H. M.; Ghareeb, M. M.; Al-Remawi, M. Therapeutic Deep Eutectic System of Capric Acid and Menthol: Characterization and Pharmaceutical Application. *J. Drug Delivery Sci. Technol.* **2019**, *53*, No. 101159.
- (37) Chalikwar, S. S.; Surana, S. J.; Goyal, S. N.; Chaturvedi, K. K.; Dangre, P. V. Solid Self-Microemulsifying Nutraceutical Delivery System for Hesperidin Using Quality by Design: Assessment of Biopharmaceutical Attributes and Shelf-Life. *J. Microencapsulation* **2021**, *38*, 61–79.

(38) Ling, J. K. U.; Chan, Y. S.; Nandong, J.; Chin, S. F.; Ho, B. K. Formulation of Choline Chloride/Ascorbic Acid Natural Deep Eutectic Solvent: Characterization, Solubilization Capacity and Antioxidant Property. *LWT* **2020**, *133*, No. 110096.

(39) Duarte, A. R. C.; Ferreira, A. S. D.; Barreiros, S.; Cabrita, E.; Reis, R. L.; Paiva, A. A Comparison between Pure Active Pharmaceutical Ingredients and Therapeutic Deep Eutectic Solvents: Solubility and Permeability Studies. *Eur. J. Pharm. Biopharm.* **2017**, *114*, 296–304.